Classroom Photocopying Permission

Chapters from Teaching General Chemistry: A Materials Science Companion. Copyright © 1993 American Chemical Society. All Rights Reserved. For reproduction of each chapter for classroom use, contact the American Chemical Society or report your copying to the Copyright Clearance Center, Inc., 222 Rosewood Drive, Danvers, MA 01923.

Experiments from Teaching General Chemistry: A Materials Science Companion. Copyright © 1993 American Chemical Society. All Rights Reserved. Multiple copies of the experiments may be made for classroom use only, provided that the following credit line is retained on each copy: "Reproduced with permission from *Teaching General Chemistry: A Materials Science Companion*." You may edit the experiments for your particular school or class and make photocopies of the edited experiments, provided that you use the following credit line: "Adapted with permission from *Teaching General Chemistry: A Materials Science Companion.*"

Overhead Masters
Multiple copies of the overhead masters may be made for classroom use only, provided that the extant credit lines are retained on each copy: "© 1993 American Chemical Society. Reproduced with permission from *Teaching General Chemistry: A Materials Science Companion*" or "© 1995 by the Division of Chemical Education, Inc., American Chemical Society. Reproduced with permission from *Solid-State Resources* ."

Laboratory Safety

DISCLAIMER

Safety information is included in each chapter of the Companion as a precaution to the readers. Although the materials, safety information, and procedures contained in this book are believed to be reliable, they should serve only as a starting point for laboratory practices. They do not purport to specify minimal legal standards or to represent the policy of the American Chemical Society. No warranty, guarantee, or representation is made by the American Chemical Society, the authors, or the editors as to the accuracy or specificity of the information contained herein, and the American Chemical Society, the authors, and the editors assume no responsibility in connection therewith. The added safety information is intended to provide basic guidelines for safe practices. Therefore, it cannot be assumed that necessary warnings or additional information and measures may not be required. Users of this book and the procedures contained herein should consult the primary literature and other sources of safe laboratory practices for more exhaustive information. See page xxv in the Text 0 Preface file in the Companion Text folder for more information.

Chapter 4

Determination of Structure Using Diffraction Data

Underpinning our understanding of the chemical and physical properties of solids is our knowledge of the structures they adopt. In this chapter, we will discuss how diffraction data is used to determine structures of crystalline materials. The same diffraction experiments that provide our window on the structures of extended solids also permit the elucidation of molecular structures, ranging from the simple (triatomic molecules like carbon dioxide) to the complex (biopolymers like proteins).

Diffraction

Atomic dimensions are on the order of angstroms (10^{-8} cm), and therefore unraveling the atomic positions of a solid requires a physical technique that operates on a similar spatial scale. The scanning tunneling microscope (STM) described in Chapters 1 and 2 provides direct images on this spatial scale but is limited to probing certain kinds of surfaces. Historically, X-ray diffraction has been the technique that has provided most of our information on the molecular-level structures of bulk solids; electron and neutron diffraction are also important techniques that obey similar physical laws *(1, 2)*. These diffraction techniques do not provide the direct atomic images accessible with the STM, but rather patterns from which atomic positions must be calculated using the physical principles of diffraction.

The role of X-rays in diffraction experiments is based on the electromagnetic properties of this form of radiation. Electromagnetic radiation is associated with electric and magnetic fields whose time-

2725-X/93/0077$06.00/1

varying magnitudes describe sine waves that are oriented perpendicular to each other and to the propagation direction. Electromagnetic radiation can thus be regarded as a wave associated with a wavelength λ and a frequency ν that obey the relationship $c = \lambda \nu$, where c is the speed of light ($\sim 3 \times 10^{10}$ cm/s in a vacuum). The wavelengths of X-rays are on the order of angstroms, or about the same length as interatomic spacings.

Maxwell von Laue recognized at the beginning of this century that X-rays would be scattered by atoms in a crystalline solid if there were a similarity in spatial scales *(1, 2)*. As illustrated in the top portion of Figure 4.1, this property leads to a pattern of scattered X-rays (the diffraction pattern) that can be mathematically related to the structural arrangement of atoms causing the scattering.

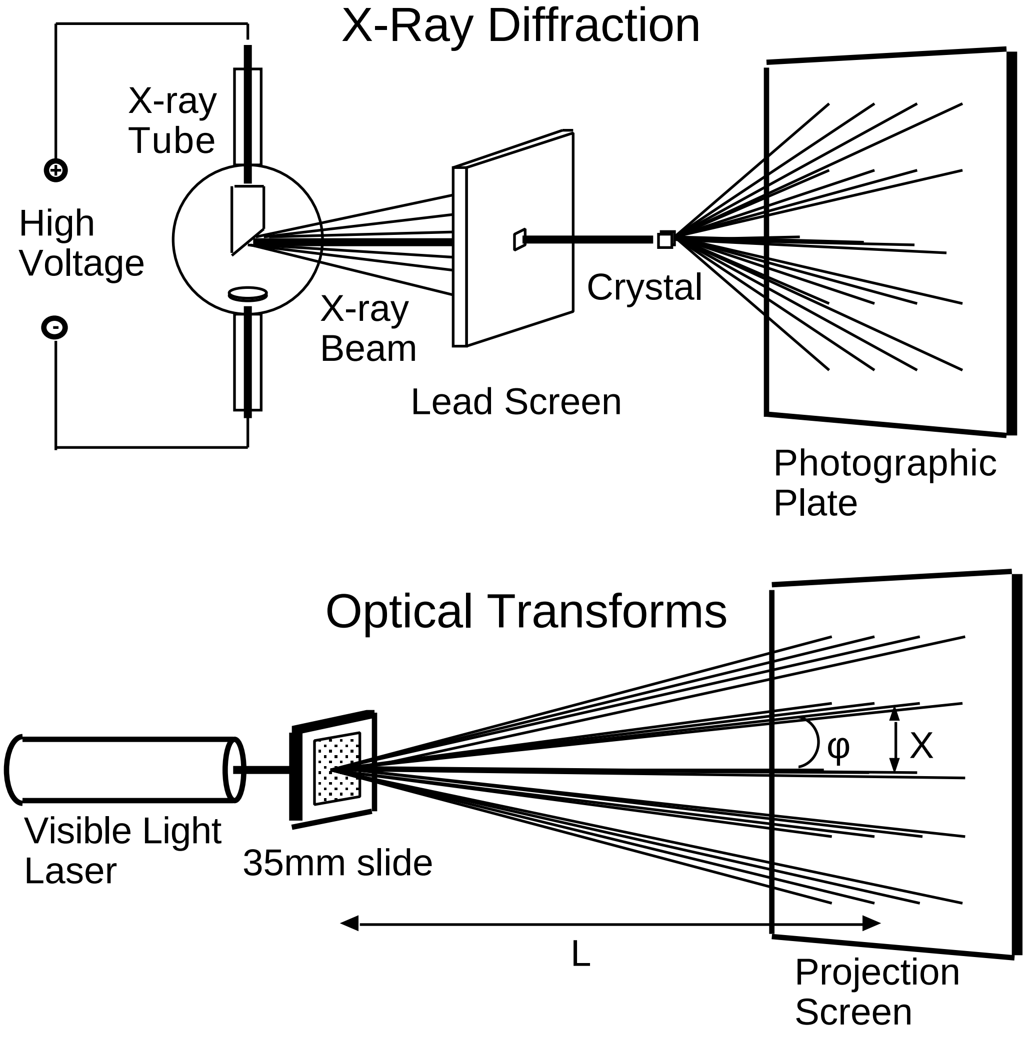

Figure 4.1. A comparison of X-ray diffraction and the optical transform.

Some time later, Sir Lawrence Bragg recognized that the experiment could be simulated inexpensively and safely by an increase in scale. He suggested the use of visible light with wavelengths thousands of times larger than those of X-rays; and arrays of dots or pinholes mimicking atomic arrangements on a scale magnified by thousands from interatomic spacings. The experiment has benefited from the technological advances of the past half-century: laser printers and lasers have superseded Bragg's heroic use of pinhole-derived patterns and multicomponent optical assemblies to produce coherent light. This kind of experiment, which yields diffraction patterns similar to X-ray diffraction patterns, is illustrated in the bottom portion of Figure 4.1, and is called an optical transform experiment. It is easily brought into the classroom or laboratory, as will be described.

The diffraction experiments shown schematically in Figure 4.1 reflect the fact that when electromagnetic radiation from several sources overlaps in space simultaneously, the individual waves add (the principle of linear superposition). The limiting cases are sketched in Figure 4.2 for two waves that are identical in amplitude, wavelength, and frequency. If the waves are in phase, reaching maximum amplitude at the same time, they reinforce one another, a condition known as constructive interference. Conversely, if the waves are completely out of phase (separated by half a wavelength, $\lambda/2$), with one at maximum amplitude while the other is at minimum amplitude, they "annihilate" one another or sum to zero, a condition known as destructive interference.

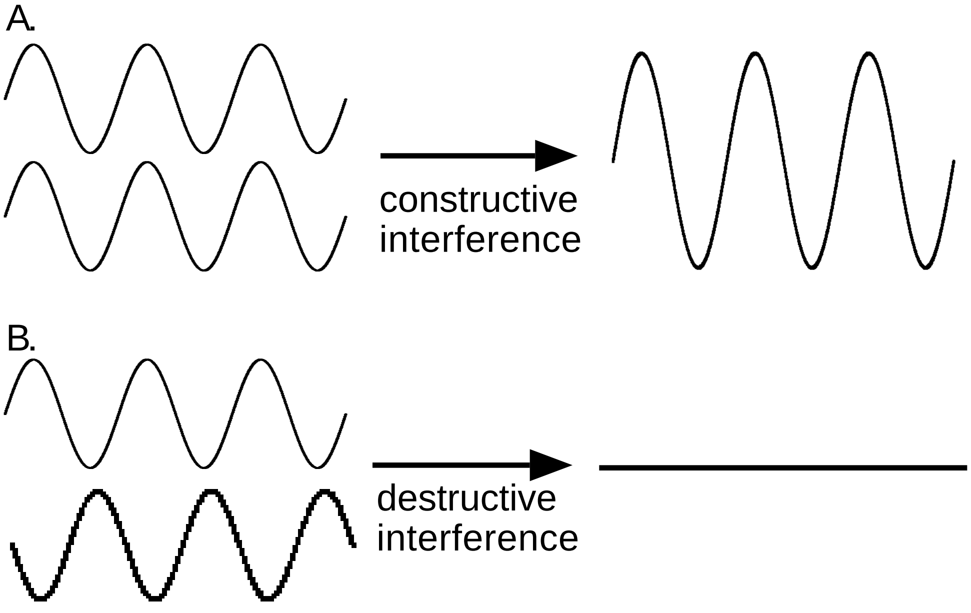

Figure 4.2. Electromagnetic radiation overlapping in space.

Exposing crystalline solids to X-rays yields diffraction patterns because the atoms in the crystal scatter the incoming radiation, and interference occurs among the many resulting waves. For most directions of observation, destructive interference will occur, but in specific directions constructive interference will be found. Electron and neutron beams also have a wavelike nature (de Broglie wavelength; $\lambda = h/mv$, where h is Planck's constant and m and v are the mass and velocity of the particle, respectively), and thus these beams lead to similar diffraction effects.

One condition for constructive interference, the Bragg diffraction condition, is illustrated in Figure 4.3 and is often described in terms of reflection from parallel planes of atoms because the angle of incidence equals the angle of diffraction. As the figure shows, if the atomic planes (represented by the rows of dots) are separated by a distance d, then X-rays reflected at a given angle θ relative to the plane will arrive at a detector in phase, if the additional distance traveled by the lower light ray relative to the upper light ray is an integral number of wavelengths, $n\lambda$ ($n = 1, 2, 3 \ldots$; $n = 1$ is called first-order diffraction, $n = 2$ is second-order diffraction, etc.). From the trigonometry indicated in Figure 4.3, this extra path length traversed by the lower light ray is $2(d \sin \theta)$, and leads to Bragg's law, $2(d \sin \theta) = n\lambda$.

Diffraction patterns thus constitute evidence for the periodically repeating arrangement of atoms in crystals. Their overall symmetry corresponds to the symmetry of the atomic packing, and the use of a single wavelength (monochromatic light) of X-ray radiation directed at the solid permits the simplest determination of interatomic distances. From the Bragg equation, it can be seen that the angle of diffraction θ is related to the interplanar spacing, d. This interplanar spacing may equal the distance between two parallel faces of a unit cell, which is the length of one edge of that unit cell. Consequently, by changing the orientation of the crystal in the X-ray beam, the lengths of all three of the edges and angles of the unit cell parallelepiped (*see* Chapter 3) can be determined. Furthermore, the intensity of the diffracted beams depends on the arrangement and atomic number of the atoms in the unit cell. Thus, the intensities of diffracted spots calculated for trial atomic positions can be compared with the experimental diffraction intensities to obtain the positions of the atoms themselves.

Bragg's version of the diffraction experiment, the optical transform experiment based on visible light, is an example of a more general phenomenon called Fraunhofer diffraction. As shown in Figure 4.3, if the light transmitted through an array of scattering centers is viewed at what is effectively infinite distance, the condition for constructive interference is $d \sin \varphi = n\lambda$, where the spacing ($d$) between atoms and scattering angle φ are defined in the figure; the scattered rays in the figure are in phase if the lower ray travels an additional distance ($d \sin \varphi$) that is an integral number of wavelengths λ. Mathematically, the equations for Fraunhofer and Bragg diffraction have a similar functional dependence on d, λ, and the scattering angle (in Bragg diffraction, the angle between the incident and diffracted beams is 2θ).

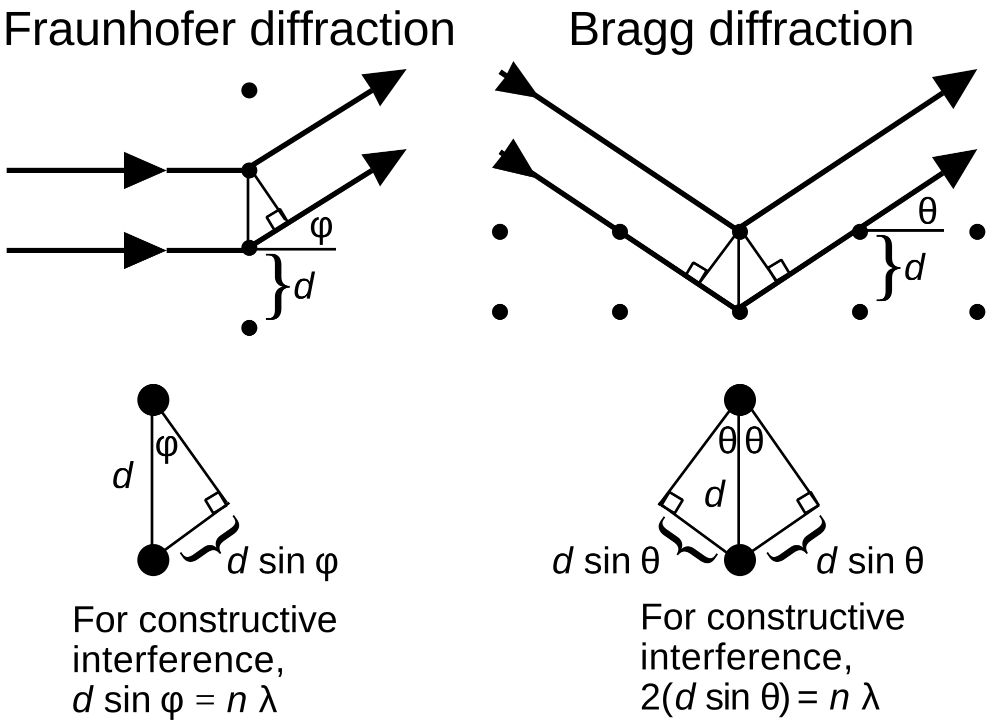

Figure 4.3. A comparison of Fraunhofer and Bragg diffraction.

Optical Transforms

The Institute for Chemical Education (ICE) makes available a set of inexpensive optical transform slides suitable for illustrating diffraction experiments, as part of an Optical Transform Kit (*see* Supplier Information for ordering information). These slides contain patterns that have been created with a laser printer (in registry with one another to permit direct comparisons of different patterns) and then photographically reduced. One such slide, a Discovery slide, contains the arrays shown in Figure 4.4. This introductory slide contains eight panels consisting of vertical lines and horizontal lines with two different spacings, and four dot patterns with the dots arranged in squares of increasing size. Figure 4.5 presents the resulting diffraction patterns obtained from each panel.

Patterns a and c of Figure 4.4 contain horizontal lines at larger and smaller separations, respectively. Each of these patterns yields a diffraction pattern of vertical spots, and by moving between these patterns (shifting the pattern relative to the light source), the viewer will note that a larger spacing between the rows on the slide results in a smaller spacing between the vertical spots in the diffraction pattern and vice versa (Figure 4.5, panels a and c).

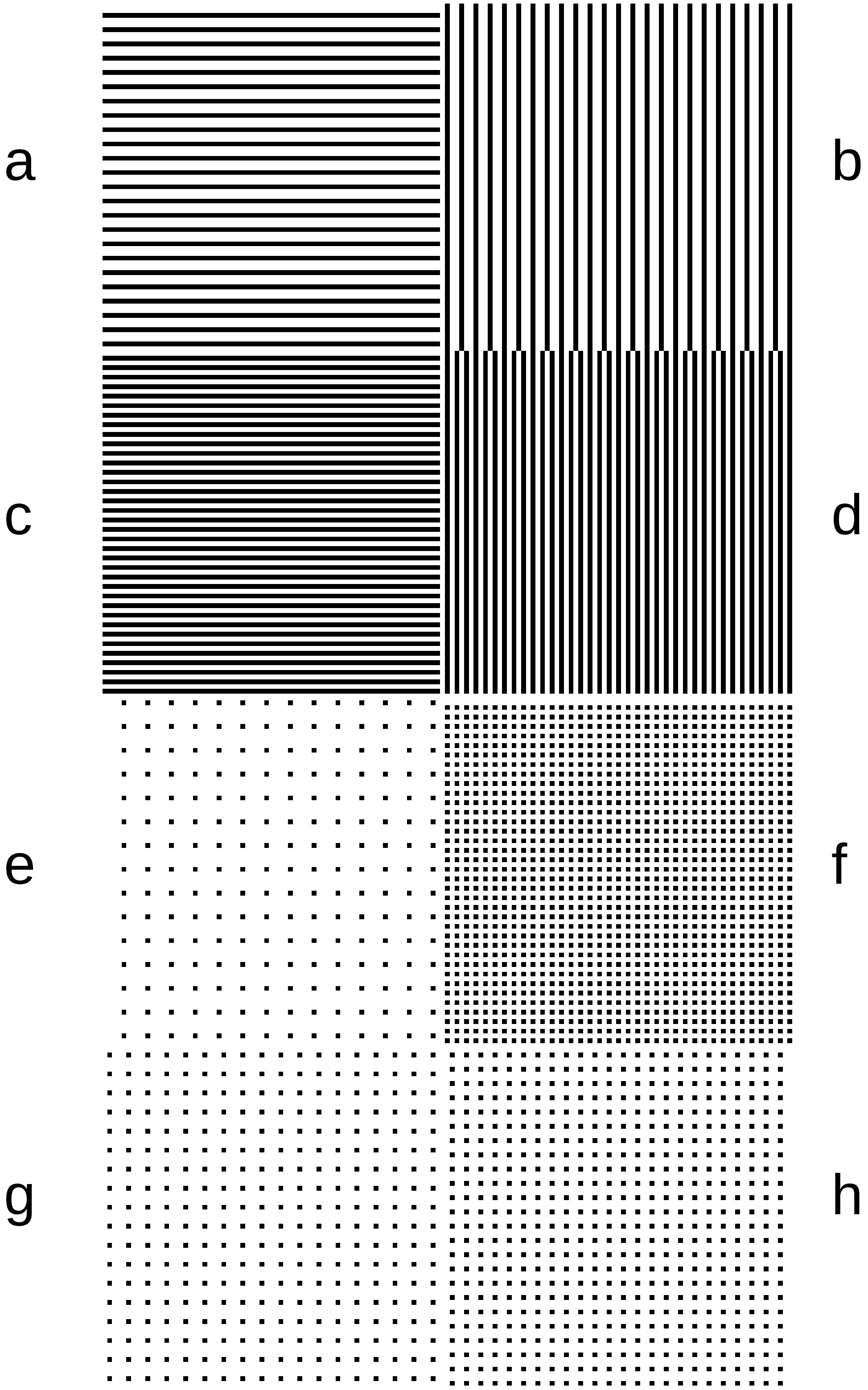

Figure 4.4. The patterns on the optical transform Discovery slide, available from ICE, oriented so that the ICE logo is on the right side as you look through the slide.

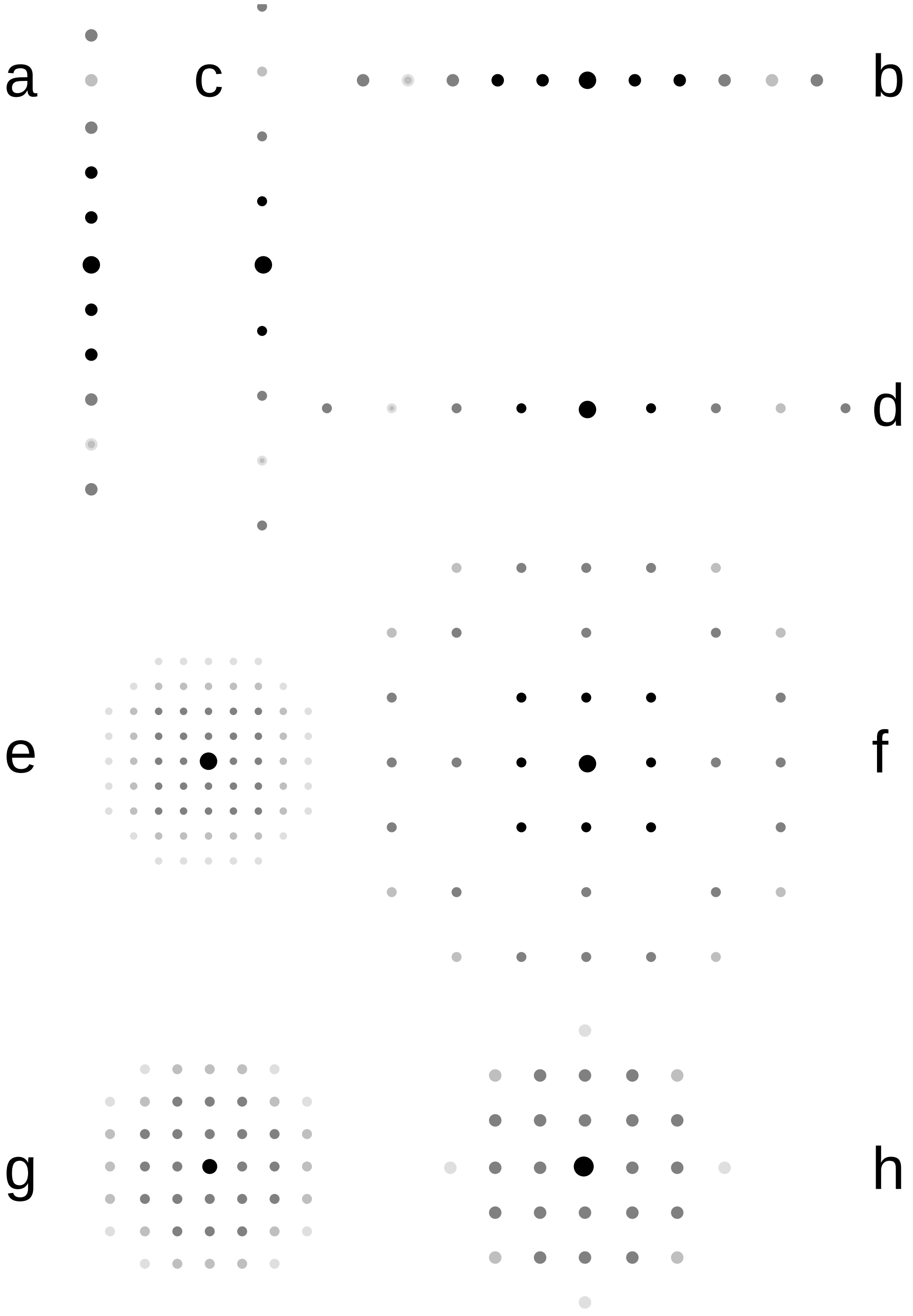

Figure 4.5. A simulation of the diffraction patterns obtained from the Discovery slide, with the indicated letter corresponding to the array (Figure 4.4) from which the diffraction pattern is produced. (The number and intensity of spots observed will vary with the intensity of light used and the darkness of the room in which the patterns are observed.)

Similarly, patterns b and d of Figure 4.4 comprise vertical lines at large and small separations, respectively, leading to a diffraction pattern of horizontal spots whose spacing varies inversely with the separation of the vertical lines on the mask (Figure 4.5, panels b and d). To lend chemical relevance to these observations, the rows and columns on the masks could be regarded as oriented polymer chains.[1]

Patterns e–h of Figure 4.4 can be viewed in rapid, counterclockwise succession, beginning with panel e (e, g, h, f), to demonstrate that as a square array of dots becomes smaller, a square diffraction pattern is also seen, whose size moves in the opposite direction, becoming largest for pattern f. Chemically, these patterns can be related to a plane of atoms in the cubic face of a simple cubic or body-centered cubic structure (Chapter 3).

The general observation illustrated by the Discovery slide is that a line of diffraction spots is seen in a direction perpendicular to and inversely spaced relative to the original rows or columns of patterns on the slide. The size of the overall diffraction pattern increases with the wavelength of light used to generate it. These findings can be amplified using other patterned 35-mm slides, as will be described later.

---

[1] The optical transform pattern produced is perpendicular to the lines in the scattering pattern. This result can be explained in the following way: Consider a pattern of horizontal lines such as those in Figure 4.4a. In the vertical direction, the repeat distance d is the separation between any two lines. Using monochromatic light, constructive interference will result when the product of the sine of the diffraction angle φ times d corresponds to a multiple (n) of the wavelength, according to the diffraction equations in Figure 4.3. Because there is a finite repeat distance in the vertical direction, there will be constructive and destructive interference in this direction.

Again considering pattern 4.4a, the repeat distance is infinite in the horizontal direction. This condition requires that $\sin \varphi$ and φ must be zero. Consequently, n must equal zero, meaning that there will be no constructive interference in the horizontal direction.

In summary, horizontal lines will result in interference in the vertical direction, and vertical lines will result in a horizontal interference pattern. Furthermore, as d becomes larger, $\sin \varphi$ (and consequently φ) must become smaller. Thus, the spacings in the transform pattern will be smaller as the repeat distance gets larger. These relationships are closely related to the notion of the reciprocal lattice in crystallography.

Demonstration 4.1. The Optical Transform Slide

Materials

Discovery slide or other optical transform slide*

Laser: A battery-powered, 5 mW, 670 nm pocket diode laser, sold as a pointer, is an effective light source and available from a number of suppliers.* For a large, darkened lecture hall, either a 10 mW, 633 nm He–Ne laser (red light) or a 0.2 mW, 544 nm He–Ne laser (green light, to which the eye is more sensitive) is effective. Both lasers are available from Melles Griot.*

Overhead transparency of the pattern on the slide (such as Figure 4.4)

Overhead projector and screen

Procedure

- In a darkened room, shine the laser light through the slide so that the diffraction pattern is displayed on a screen at a distance of several meters from the source. The laser should be clamped or taped in a fixed position. **CAUTION: Take care to ensure that the viewers will not inadvertently look directly at the beam where it emerges from the laser. Clamp or tape the laser in a fixed position so that the beam will not accidentally shift. Aiming a laser at a person or looking directly at a source of laser light can be harmful to the eye!**
- Each slide contains eight patterns. Move the slide so that it intercepts the beam in different places. This procedure will allow the patterns to be displayed in order according to preference. Simultaneous display of the overhead transparency containing the enlarged image pattern will allow the pattern of diffraction spots to be discussed in light of the array of dots that generated them. Some comparisons that can be made:
- Shine the laser through patterns a and c of Figure 4.4. This will show the effect of varying the spacings of horizontal lines on the diffraction pattern.
- Shine the laser through patterns b and d of Figure 4.4. This will show the effect of varying the spacings of vertical lines on the diffraction pattern.
- Shine the laser sequentially through patterns e, g, h, and f of Figure 4.4. This will show the effect of changing the size of a square unit cell of dots on the diffraction pattern.

**See* Supplier Information.

Demonstration 4.2. Individualized Use of Optical Transform Slides

Materials

Optical transform slides, one for each person in the class (ICE sells the optical transform slides in bulk. *See* Supplier Information.)
Laser (*see* Demonstration 4.1)
Point source of white light (a small flashlight bulb or miniMaglite—a small flashlight that is available at camping or hardware stores—with the lens unscrewed)
Magnifying glass or hand-held lens (a 30× Micronta Microscope from Radio Shack works well) (optional)

Procedure

- Make a 35 mm optical transform slide available to each class member. In addition to having the instructor provide an enlarged view of the slide's contents, a small magnifying glass, hand-held lens, or microscope can be used to verify the patterns on the slide.
- Have the students visually orient their slides by noting the relative transparency of different regions (patterns c and d of Figure 4.4, with the densest packing of lines, will appear darkest, for example).
- Project a laser beam on the screen (without passing it through a slide). **CAUTION: Take care to ensure that the viewers will not inadvertently look directly at the beam where it emerges from the laser. Clamp or tape the laser in a fixed position so that the beam will not accidentally shift. Aiming a laser at a person or looking directly at a source of laser light can be harmful to the eye!**
- Have the students view the laser spot through their own 35-mm slides at a distance of at least a few meters from the screen. The diffraction pattern is observed and can be changed at the viewers' convenience as they view the beam through different portions of the slide. Thus, the same diffraction pattern appears whether the laser beam passes through the slide and off a projection screen to reach the eye (*see* previous demonstration), or whether the laser beam bounces off the projection screen and then through the slide to reach the eye.
- Hold a point source of white light such as the miniMaglite in front of the projection screen. Ask students to view the light through their slides. Instead of seeing monochromatic diffraction spots, as observed when the laser is used, each diffraction spot is dispersed into the colors of the visible spectrum to give a dramatically colorful effect. This latter viewing technique demonstrates that the slide patterns are indeed diffraction gratings.

To quantitatively verify the Fraunhofer relationship directly, any of the patterns in Figure 4.4 may be used. As depicted in Figure 4.1, the size or spread of the diffraction pattern is reflected in the value of tan φ, which can be calculated by trigonometry from the spot spacing in the diffraction pattern X and the distance between the pattern and the slide L, that is, $\tan \varphi = X/L$; the value of φ is sufficiently small in this experiment that tan φ can be well approximated as φ (in radians) so that $\varphi = X/L$. Knowing λ, the diffraction equation can then be used to calculate d and to compare it with the known values.[2] Or, assuming that the array spacing d is known, λ can be calculated. Because sin φ is also approximately equal to φ (measured in radians) for the small angles observed in this experiment, φ should be roughly proportional to λ.

The relationship can be demonstrated qualitatively by using the white light source described: each diffracted spot contains the full visible spectrum, with red at the greatest distance from the center (the largest diffracted angle φ) and violet at the shortest distance from the center (the smallest diffracted angle φ). If several different lasers are available (like red and green He–Ne lasers), the quantitative form of the Fraunhofer equation can be experimentally verified at each wavelength.

In contrast to the direct relationship between sin φ and λ, d and sin φ should be inversely related from the Fraunhofer equation. Indeed, the comparisons of panel a with c; of panel b with d; and of panels e through h all demonstrate that as the spacing between lines or dots on the masks diminishes, the size of the diffraction pattern increases.

Laboratory. A laboratory experiment that explores X-ray diffraction using the optical transform slides is described in Experiment 4. A second experiment uses X-ray data to determine the interlayer spacing in a layered solid (Experiment 5).

In addition to the optical transform experiments already described, several other slides are available from ICE. Figure 4.6 displays eight additional arrays of laser-printer-written, photographically-reduced dots, and Figure 4.7 presents the corresponding diffraction patterns. Although these arrays are two-dimensional, they mimic what would be observed for diffraction from particular three-dimensional structures that are viewed in projection perpendicular to a face that is a parallelogram. For example, Figures 4.6b and 4.6d are the arrays of atoms in the sc structure and the projection of a fcc structure; the centered array of Figure 4.6a mimics the projection of a bcc structure and a projection of the diamond structure

---

[2] The patterns are drawn pixel-by-pixel and printed on a laser printer. The actual size of the pattern may vary slightly from one slide to another because each 35-mm slide is shot individually. The size of the pixel (x) is about 0.030 mm on the slide. Thus, in Figure 4.4, the repeat distance in patterns c, d, and f is $2x$; in a, b, and h, $3x$; in g, $4x$; and in e, $5x$.

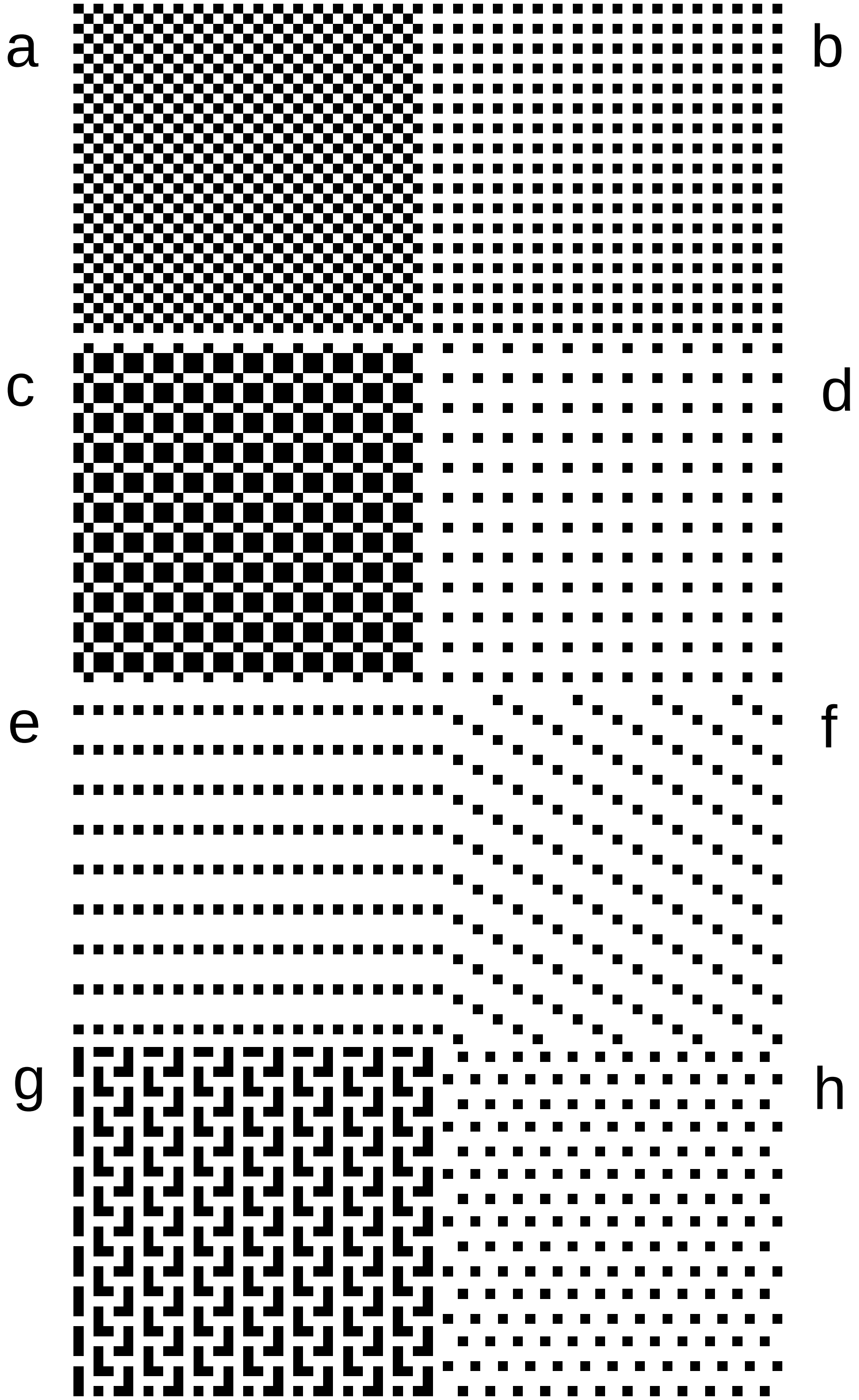

Figure 4.6. The patterns on the optical transform Unit Cell slide, available from ICE, (oriented so that the ICE logo is on the right side as you look through the slide).

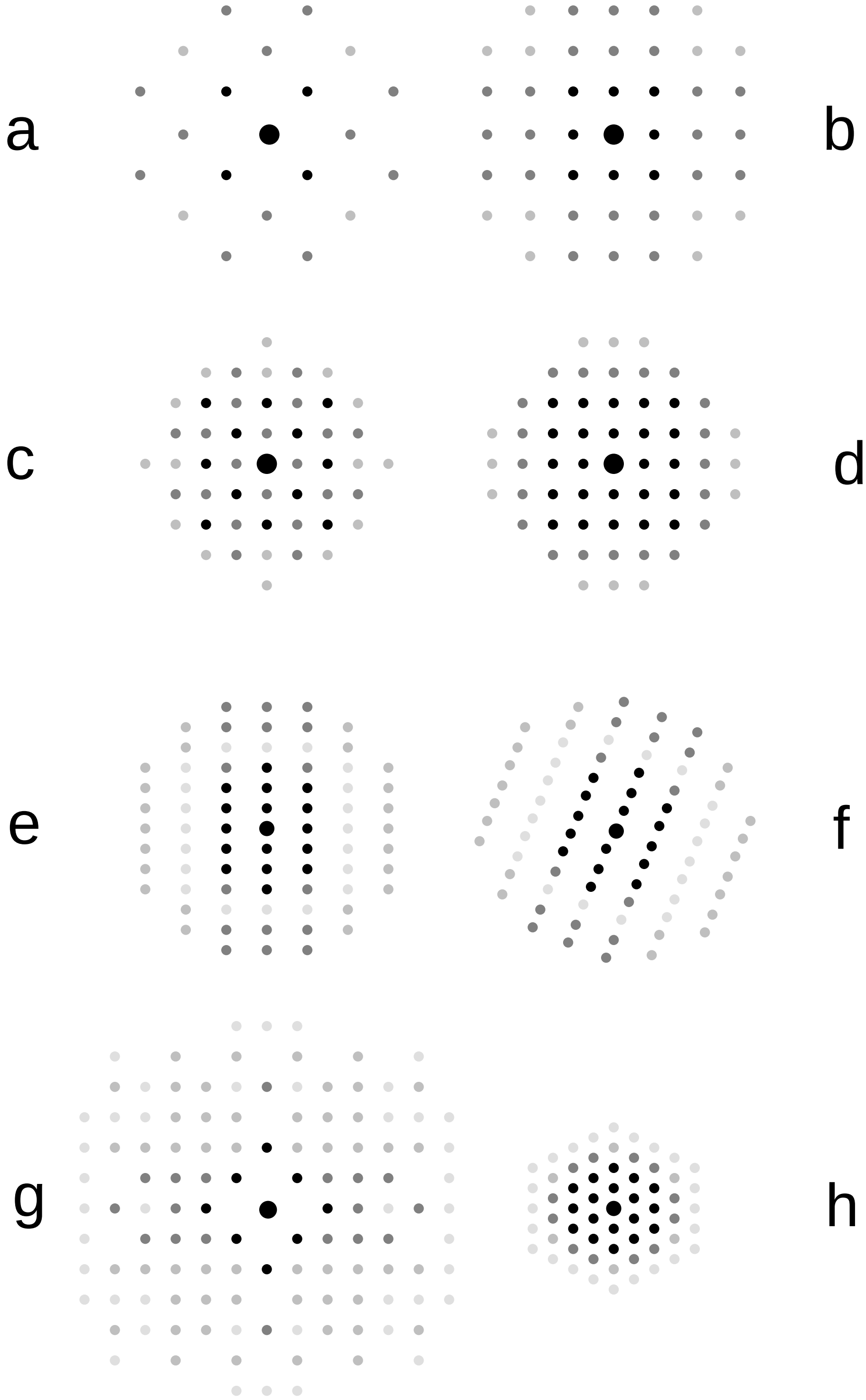

Figure 4.7. A simulation of the diffraction patterns from Figure 4.6. The letters correspond to the array from which the diffraction pattern is derived.

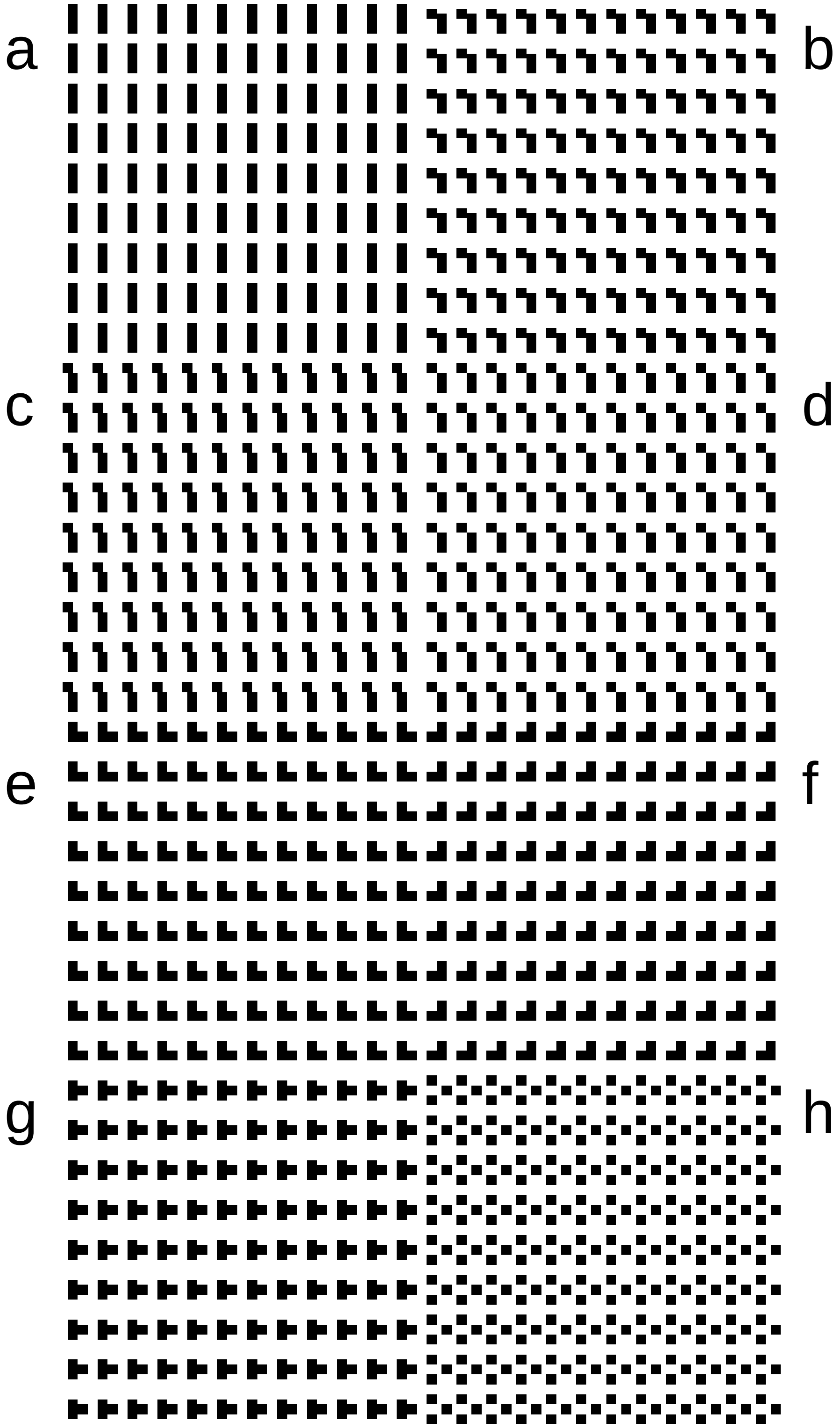

Figure 4.8. The patterns the optical transform VSEPR slide, available from ICE, (oriented so that the ICE logo is on the right side as you look through the slide).

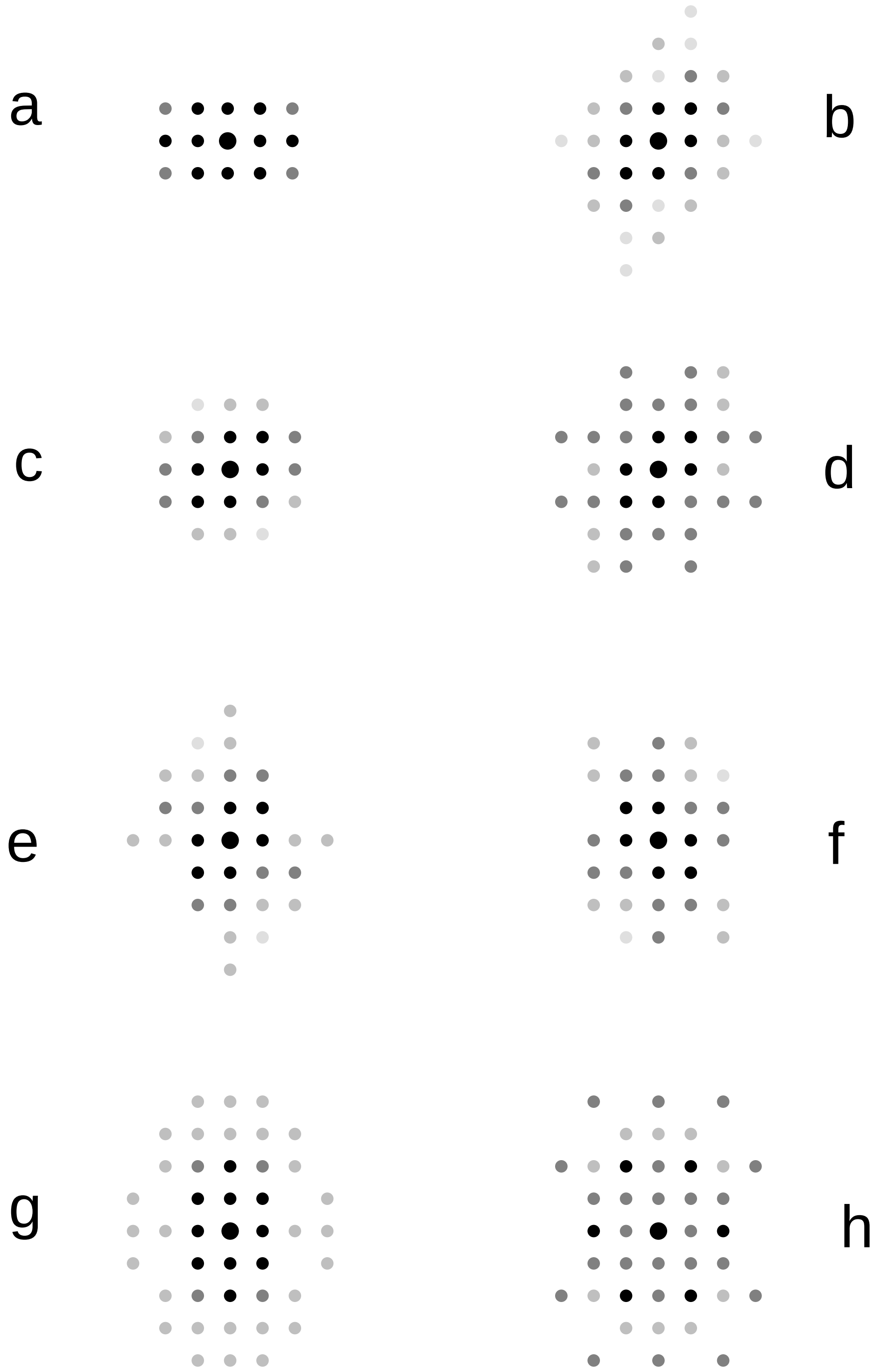

Figure 4.9. A simulation of the diffraction patterns from Figure 4.8. The indicated letter corresponds to the array from which the diffraction pattern is produced.

(Chapter 5); the array of Figure 4.6c simulates the projection of the cubic zinc blende structure (Chapter 5), having two different kinds of atoms, each surrounded by four atoms of the other type in a tetrahedral arrangement (this is also the array that would be seen for a single layer of the NaCl rock salt structure).

Comparison of the diffraction patterns from Figures 4.6a and 4.6b shows the effects of placing an identical atom in the center of the unit cell (every other diffraction spot is eliminated, Figures 4.7a and 4.7b), while comparison of Figures 4.6c and 4.6d shows the effects of placing a different atom in the center of the unit cell (every other diffraction spot is changed in intensity, Figures 4.7c and 4.7d). Additional examples include the rectangular structures of Figure 4.6e and 4.6g which are derived from so-called orthorhombic unit cell structures, wherein all angles are 90°, but the sides are of unequal length; the array of Figure 4.6f mimics a so-called monoclinic structure, where a non-90° angle is in the plane of the paper. Note the change in orientation between the unit cell and its diffraction pattern, where the long direction becomes the short direction and the short direction becomes the long direction. Figure 4.6h is a closest-packing structure, the basis for layers of hexagonal close-packed (hcp) and cubic close-packed (ccp) structures (Chapter 5). Finally, diffraction arising from the packing of L-shaped molecules related by glide symmetry (the symmetry of footprints on a beach) is illustrated by Figure 4.7g.

Also available from ICE is a slide for illustrating how molecular geometries are determined, which is meant to complement discussions of the valence-shell electron-pair repulsion (VSEPR) rules used to predict molecular structures. This slide and its corresponding diffraction patterns, Figures 4.8 and 4.9, simulate molecular solids comprised exclusively of triatomic molecules. The molecular shapes correspond to bond angles ranging from 180° (array a) down through about 60° (array h). The unit cell for all of these arrays is identical, a rectangle of 3 × 4 picture elements (pixels).

The diffraction patterns that result from these arrays all have the same geometry and reflect the size of the unit cell they have in common. However, the relative intensities of the different diffracted spots vary substantially and produce strikingly different patterns. The point can be made that the overall symmetry of the diffraction pattern reveals the symmetry of the molecular packing, and the relative intensities of the spots can be analyzed to determine the molecule's structure.

References

1. Laue, M. *Sitzungsber. Kais. Akad. Wiss., München* **1912**, *1912*, 263.
2. Schwartz, L. H.; Cohen, J. B. *Diffraction from Materials*, 2nd ed.; Springer-Verlag; New York, 1987.
3. Lisensky, G. C.; Kelly, T. K.; Neu, D. R.; Ellis, A. B. *J. Chem. Educ.* **1991**, *68*, 91–96.

Additional Reading

- Harburn, G.; Taylor, C. A.; Welberry, T. R. *Atlas of Optical Transforms*; Cornell University Press: Ithaca, NY, 1975.
- Taylor, C. A.; Lipson, H. *Optical Transforms*; Cornell University Press: Ithaca, NY, 1964.
- Welberry, T. R.; Thomas, J. M. *Chem. Br.* **1989**, 383–388.

Acknowledgments

This chapter is based in part on reference 3 and on discussions with Richard Matyi and Thomas Kelly, University of Wisconsin—Madison, Department of Materials Science and Engineering.

Exercises

1. What is the frequency of an X-ray with a wavelength of 1.54 Å, the wavelength produced by an X-ray tube with a copper target? (The speed of light is 2.998×10^8 m/s). What is the frequency of an X-ray with a wavelength of 0.7107 Å, the wavelength produced by an X-ray tube with a molybdenum target?

2. What is the angle of the second-order diffraction ($n = 2$) of 1.54-Å X-rays, the wavelength produced by an X-ray tube with a copper target, from each of the following sets of planes? (a is the length of the cubic unit cell)
   a. The unit cell faces of CsCl, $a = 4.123$ Å
   b. The unit cell faces of NaCl, $a = 5.6406$ Å
   c. The unit cell faces of Po, $a = 3.35$ Å
   d. The unit cell faces of Na, $a = 4.291$ Å
   e. The unit cell faces of Ni, $a = 3.524$ Å

   (Alternate questions could use any of the data in Appendix 5.6, or could use 0.7107-Å X-rays, the wavelength produced by an X-ray tube with a molybdenum target.)

3. What is the angle of first-order diffraction ($n = 1$) of 1.54-Å X-rays from the sets of closest-packed planes in each of the following metals?
   a. Be (layer spacing $d = 1.79$ Å)
   b. Cd ($d = 2.809$ Å)
   c. Mg ($d = 2.60$ Å)
   d. Ni ($d = 2.16$ Å)
   e. Zn ($d = 2.473$Å)

4. First-order diffraction ($n = 1$) is observed from the closest-packed planes of the following metals. If 1.54-Å X-rays were used in the diffraction study, determine the spacing between the closest-packed planes from the given diffraction angles.
   a. Be ($\theta = 25.48°$)
   b. Cd ($\theta = 15.91°$)
   c. Mg ($\theta = 17.23°$)
   d. Ni ($\theta = 20.88°$)
   e. Zn ($\theta = 18.14°$)

5. What is the frequency of a 670 nm laser?

6. Sketch a unit cell of any of the patterns in Figures 4.6 and 4.8.

7. Sketch a qualitative representation of the diffraction pattern produced by the following two-dimensional arrays.

a.

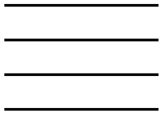

b.

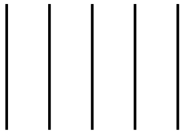

c.

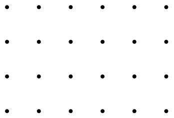

8. Sketch a qualitative representation that shows the difference in the diffraction pattern produced by the following pairs of two-dimensional arrays.

a.

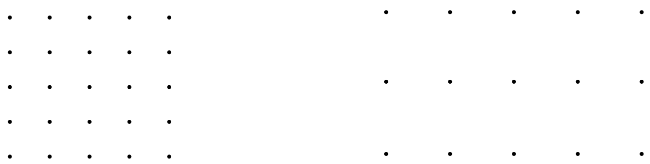

b.

c.

d.

9. The two arrays of dots, **a** and **b** are identical except that in array **b** there is an extra dot in the middle of each rectangle formed by four neighboring dots in array **a**.

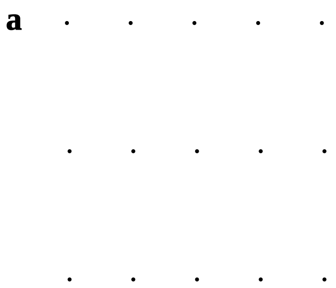

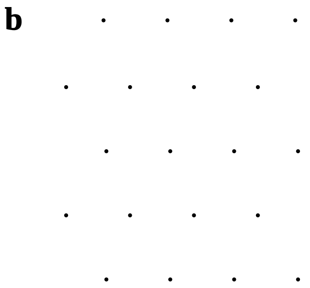

The diffraction patterns are identical except that every other diffraction spot is missing from one of the patterns, as follows:

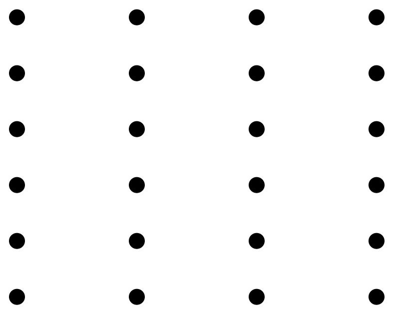

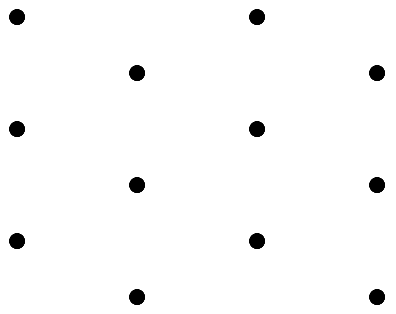

a. Which of the two diffraction patterns above corresponds to array **a** and which to array **b**?
b. Explain why having twice as many dots (array **b** relative to array **a**) in the array has the effect you describe in part a on the diffraction pattern.
c. Interpret the change in diffraction patterns in going from array **a** to array **b** in terms of the unit cells of the two arrays.

10. Infrared light and ultraviolet light can be used to generate a diffraction pattern from an array like that in Exercise 7a. If your eyes were sensitive to infrared (IR) light with a wavelength of 8000 Å and to ultraviolet (UV) light with a wavelength of 3000 Å, what difference would you see in the patterns generated with these two types of light?

11. Why must X-rays be used in crystal-structure determinations rather than visible light?

12. Why does X-ray diffraction give more information about the three-dimensional structure of a crystalline solid than does scanning tunneling microscopy?

13. A student is using an optical transform slide and is attempting to determine the spacing between images on the slide. If she is using a red He–Ne laser (λ = 633 nm) and is standing 6.0 meters from the projection screen, the distance from the large center spot to the nearest diffraction spot is 3.8 cm. What is the spacing between images on the slide?

14. Use the Bragg equation to explain the observation that as the spacing between atoms decreases, the spacings in the resulting diffraction pattern increase.

15. The X-ray diffraction patterns from a crystal oriented to view the diffraction from a face of the cubic unit cell are shown.

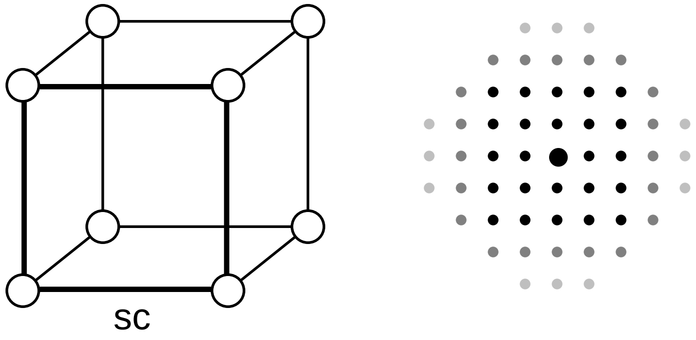

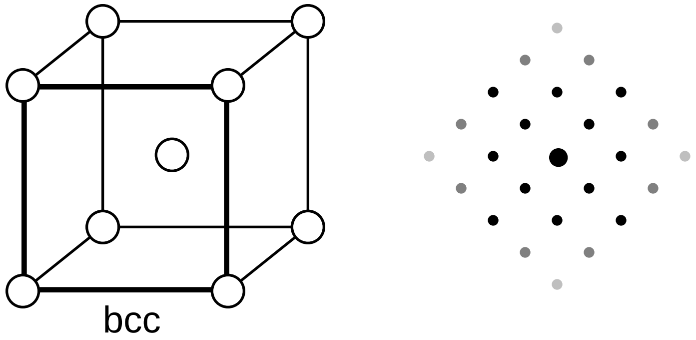

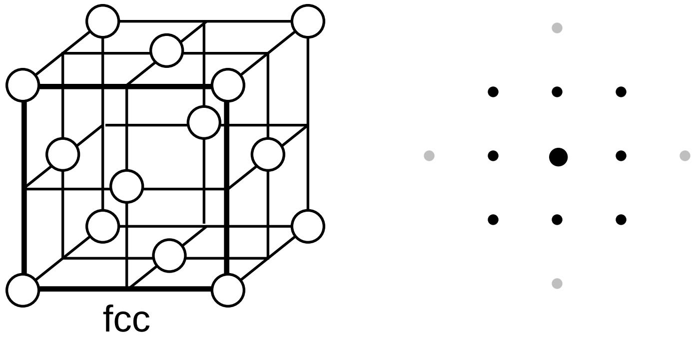

a. What happens to the diffraction spot pattern in moving from simple cubic to body-centered cubic or face-centered cubic?
b. Predict the diffraction patterns for the same orientation of CsCl and Cu_3Au.